J|A|C|S COMMUNICATIONS

Published on Web 02/12/2009

# Oxygen Vacancy Clusters Promoting Reducibility and Activity of Ceria Nanorods

Xiangwen Liu,[†,§] Kebin Zhou,*[,†] Lei Wang,[†] Baoyi Wang,[‡] and Yadong Li*[,§]

*College of Chemistry and Chemical Engineering, Graduate University of the Chinese Academy of Sciences, Beijing, 100049, P. R. China, Institute of High Energy Physics, Chinese Academy of Sciences, Beijing, 100049, P. R. China, and Department of Chemistry, Tsinghua University, Beijing, 100084, P. R. China*

Received October 27, 2008; E-mail: kbzhou@gucas.ac.cn; ydli@tsinghua.edu.cn

Ceria, a catalytic material, has attracted much attention in recent years.[1] The importance of ceria in catalysis originates from its remarkable redox and oxygen storage capability (OSC) in automobile exhaust converters. It can undergo repeatable $Ce^{4+}/Ce^{3+}$ redox cycles depending on the conditions in the exhaust stream.[2] In fact, the actual importance of oxygen uptake/release is determined by not only the OSC but also the rates of the redox cycles. However, while the rate of cerium oxidation is much faster, reduction of ceria is generally sluggish. Thus, great effort has been made to promote its reducibility.[3] As discussed in these studies, the reduction of ceria is proposed to be controlled by the nature of the oxygen vacancies, since oxygen diffusion, the rate-controlling step, depends on the type, size, and concentration of oxygen vacancies.[4] For example, Esch et al. showed that small size surface oxygen vacancies on $CeO_2$ (111) were immobile at room temperature, but linear clusters of these vacancies formed at higher temperatures.[4a] This indicates that any processing condition which favors the formation of more desired oxygen vacancies will result in enhanced reducibility. Thus the precise role of oxygen vacancies is crucial to the greater understanding of these important oxide materials. However, creating these favorable defects and understanding their roles in the reducibility and activity of nanosized ceria at the atomic level is still lacking.

Here, two ceria nanorod (NR) samples with different types and distributions of oxygen vacancies were synthesized. The results show direct evidence of promoting the reducibility and activity of ceria NRs with a high concentration of larger size oxygen vacancy clusters.

One ceria sample (ceria-A) enriched with larger size oxygen vacancy clusters was prepared by a hydrothermal method using $CeCl_3$ as a cerium precursor. The other sample (ceria-B) with fewer larger size defects was prepared by the same method except employing $Ce(NO_3)_3$ as the cerium precursor. XRD analysis (Figure S1) revealed that both of the prepared materials could be indexed to the pure fluorite cubic structures (JCPDS 34-0394). TEM images (Figure 1A, B) of the products revealed that the two ceria samples showed rodlike morphologies, 100−300 nm in length and ∼12−20 nm in diameter. The BET surface area of the as-prepared ceria-A and -B was 51.5 and 60.4 $m^2/g$, respectively.

The catalytic activities of the materials were investigated by performing the CO oxidation reaction. The "light-off" reaction profiles (Figure S2) showed that ceria-A was much more active than ceria-B. When the reaction was carried out at 160 °C under steady state conditions, the specific rate of ceria-A was 0.51 $\mu$mol $g^{-1}_{cat}$ $s^{-1}$, while that of ceria-B was only 0.21 $\mu$mol $g^{-1}_{cat}$ $s^{-1}$ (Figure 1C). These results were reproduced numerous times with several preparative batches of ceria-A and -B.

To reveal fundamental reasons for these phenomena, HRTEM analysis were performed. The results (Figures 1D, F and S3) reveal

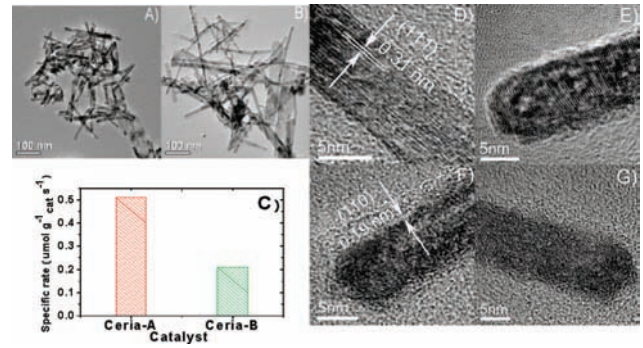


***Figure 1.*** (A) TEM images of ceria-A. (B) TEM images of ceria-B. (C) Graph showing the specific rate for CO oxidation on ceria. Reaction conditions: the molar ratio for CO/air/$N_2$ was 1:16:83, with a contact time (W/F) of 75 $g_{cat}$ h $mol_{CO}^{-1}$; reaction temperature 160 °C. (D, E) HRTEM images of ceria-A. (F, G) HRTEM images of ceria-B.

that ceria-A predominantly exposes the {100} and {111} planes, whereas the {100} and {110} planes are predominantly exposed in ceria-B (see Supporting Information). Theoretical studies have shown that {111} is the least active surface, followed by {100} and {110}.[5] However, the results of activity evaluation showed that ceria-A was more active than ceria-B for CO oxidation. This indicates that, besides the reactivity of crystal planes, there are other factors for determining the ceria activity. Through careful observation of these HRTEM images of ceria NRs, it was found that there were many "dark pits" on ceria-A (Figures 1E and S4), while there were fewer on ceria-B (Figures 1G and S4). This revealed the surfaces of the former were rougher than those of the latter, indicating more surface reconstruction occurred on ceria-A. From these results, we speculate that defects in the ceria may be an important factor that will prove useful.

X-ray photoelectron spectra analysis was carried out to characterize the valence state of Ce ions. Although most of the Ce ions were $Ce^{4+}$, the presence of $Ce^{3+}$ was clearly revealed in both ceria-A and -B (Figures 2A, S6−S8 and discussions). In addition, lattice expansion as revealed through XRD analysis (Figure S10) provides more evidence for the existence of $Ce^{3+}$ in these materials.[6] It is well-known that once $Ce^{3+}$ appears in the fluorite ceria, oxygen vacancies will be generated to maintain electrostatic balance according to the following:[7]

$$4Ce^{4+} + O^{2-} \rightarrow 4Ce^{4+} + 2e^-/\square + 0.5O_2 \rightarrow 2Ce^{4+} + 2Ce^{3+} + \square + 0.5O_2 \quad (1)$$

where □ represents an empty position (anion-vacant site) originating from the removal of $O^{2-}$ from the lattice, here represented as an oxygen tetrahedral site ($Ce_4O$).

Positron annihilation spectrum is a well established technique to study defects in materials. The lifetime of the positron is able to give

[†] Graduate University of the Chinese Academy of Sciences.
[‡] Chinese Academy of Sciences.
[§] Tsinghua University.



10.1021/ja808433d CCC: $40.75 

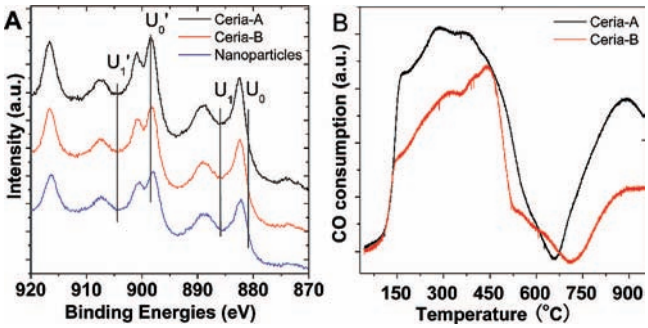


***Figure 2.*** (A) Ce3d XPS spectra from ceria-A, ceria-B, and ceria nanoparticles mainly with $Ce^{4+}$ for comparison. Four peaks labeled as $u_0$/$u_0'$ and $u_1$/$u_1'$ were identified for $Ce^{3+}$ 3d final states. (B) CO-TPR profiles of ceria-A and ceria-B.

***Table 1.*** Position Lifetime Parameters of Ceria-A and Ceria-B

| sample | $\tau_1$ (ps) | $\tau_2$ (ps) | $\tau_3$ (ns) | $I_1$ (%) | $I_2$ (%) | $I_3$ (%) |
|---|---|---|---|---|---|---|
| ceria-A | 236 | 408 | 3.56 | 38.9 | 60.4 | 0.7 |
| ceria-B | 247 | 547 | 1.94 | 65.8 | 28.1 | 6.1 |

information about the size, type, and relative concentration of various defects/vacancies even at the ppm level. The positron lifetime spectra of both ceria-A and -B yielded three distinct lifetime components, $\tau_1$, $\tau_2$, and $\tau_3$, with relative intensities $I_1$, $I_2$, and $I_3$ (Table 1 and Figure S11). The longest component ($\tau_3$) was due to the annihilation of orthopositronium atoms formed in the large voids present in the material.[8] The shortest one ($\tau_1$) was attributed to small neutral $Ce^{3+}$-oxygen vacancy associates, probably in the form of $Ce'_{Ce}V_O^{\cdot\cdot}Ce'_{Ce}$. Compared with bulk ceria,[8c] another component ($\tau_2$), 400−550 ps, was observed. This component could be assigned to larger size defects in the materials, such as vacancy clusters in $SiO_2$ and congeries of the $\tau_1$ type vacancies in ZnO.[8b,d] Thus larger size oxygen vacancy clusters (i.e., dimmers, trimers, or larger), resulting from interaction between the small neutral $Ce^{3+}$-oxygen vacancy associates ($\tau_1$), were assigned to the $\tau_2$ component. Besides the lifetime of the positron, its relative intensity ($I$) gave more information on the distribution of these defects since the relative intensity quantifies the abundance of that vacancy with respect to some standard of the same material. In ceria-A, $I_2 > I_1$, indicating higher concentration of larger size oxygen vacancy clusters than small neutral vacancy associates in this material. However, a reverse trend was found in ceria-B; that is, isolated vacancy associates are predominate.

It is widely accepted that the migration of oxygen in ceria and ceria-based materials takes place via a vacancy hopping mechanism.[9] Clusters of more than two vacancies, such as linear surface oxygen vacancies, proved to be favorable for migration of oxygen.[4a] If the diffusion of anions is sufficiently fast, a continuous supply of oxygen from the bulk to the surface will guarantee an enhanced reducibility. Thus ceria-A with a higher concentration of larger size oxygen vacancy clusters should be more reducible than ceria-B. The reducibility was characterized by temperature-programmed reduction (CO-TPR). The typical two peak reduction profiles are shown in Figure 2B. The low-temperature peak (<600 °C) is of particular interest since it is related to the surface oxygen reduction. The amount of oxygen that can be attracted from the surface of ceria-A is ∼1.36 times that of ceria-B. This confirms our predication that the reducibility of ceria can be enhanced by the larger size oxygen vacancy clusters. More significantly, abstraction of oxygen from the surface of ceria-A mostly occurred at low temperature ranges (150−450 °C), indicating there are more available reactive oxygen species on the surface of ceria-A.

***Scheme 1.*** Catalytic Pathway for CO Oxidation over Ceria Nanorods Enriched with Larger Oxygen Vacancy Clusters

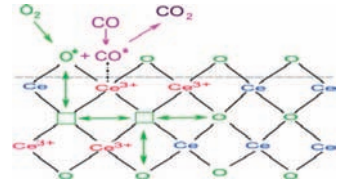


Thus a catalytic pathway (Scheme 1) is proposed for CO oxidation on these defective ceria NRs, which involves alternative reduction and oxidation of the ceria surface with formation of oxygen vacancies and their successive replenishment by gas-phase oxygen. The presence of oxygen vacancy clusters facilitates the activation and transportation of active oxygen species. Furthermore, these vacancy clusters expose exclusively $Ce^{3+}$ ions, providing effective adsorption sites to gas phase carbon monoxide.[4b] Therefore, it was the larger vacancy clusters coupled with the adjacent $Ce^{3+}$ ions that guaranteed the promoting reactivity of the ceria-A sample.

In summary, two types of oxygen vacancies, small neutral $Ce^{3+}$-oxygen vacancy associates and larger size clusters of these defects, were discovered in the ceria NRs. The synthesis method was crucial to determine their distribution. A direct relationship between the concentration of the larger size oxygen vacancy clusters and the reducibility and reactivity of nanosized ceria was revealed. These results may be a primary step in understanding and designing active sites at the surface of metal oxide catalytic materials.

**Acknowledgment.** This work was supported by NSFC (20703065, 20877097), 863 Program (2008AA06Z324), and the State Key Project of Fundamental Research for Nanoscience and Nanotechnology (2006CB932303).

**Supporting Information Available:** Experiment details of synthesis, HRTEM, XPS, XRD, XRF, and relevant discussion. This material is available free of charge via the Internet at http://pubs.acs.org.

## References

(1) Wang, R.; Crozier, P. A.; Sharma, R.; Adams, J. B. *Nano Lett.* **2008**, *8*, 962. (b) Si, R.; Flytzani-Stephanopoulos, M. *Angew. Chem.* **2008**, *120*, 2926; *Angew. Chem., Int. Ed.* **2008**, *47*, 2884. (c) Simonsen, S. B.; Dahl, S.; Johnson, E.; Helveg, S. *J. Catal.* **2008**, *255*, 1.
(2) Trovarelli, A. *Catal. Rev.-Sci. Eng.* **1996**, *38*, 439.
(3) (a) Zhao, M. W.; Shen, M. Q.; Wang, J. *J. Catal.* **2007**, *248*, 258. (b) Dutta, G.; Waghmare, U. V.; Baidya, T.; Hegde, M. S.; Priolkar, K. R.; Sarode, P. R. *Chem. Mater.* **2006**, *18*, 3249. (c) Yamamoto, T.; Suzuki, A.; Nagai, Y.; Tanabe, T.; Dong, F.; Inada, Y.; Nomura, M.; Tada, M.; Iwasawa, Y. *Angew. Chem.* **2007**, *119*, 9413. (d) Zhou, K. B.; Wang, X.; Sun, X. M.; Peng, Q.; Li, Y. D. *J. Catal.* **2005**, *229*, 206. (e) Aneggi, E.; Llorca, J.; Boaro, M.; Trovarelli, A. *J. Catal.* **2005**, *234*, 88. (f) Sayle, D. C.; Feng, X. D.; Ding, Y.; Wang, Z. L.; Sayle, T. X. T. *J. Am. Chem. Soc.* **2007**, *129*, 7924.
(4) (a) Esch, F.; Fabris, S.; Zhou, L.; Montini, T.; Africh, C.; Fornasiero, P.; Comelli, G.; Rosei, R. *Science* **2005**, *309*, 752. (b) Campbell, C. T.; Peden, C. H. F. *Science* **2005**, *309*, 713. (c) Dutta, P.; Pal, S.; Seehra, M. S.; Shi, Y.; Eyring, E. M.; Ernst, R. D. *Chem. Mater.* **2006**, *18*, 5144.
(5) Sayle, T. X. T.; Parker, S. C.; Catlow, C. R. A. *Surf. Sci.* **1994**, *316*, 329.
(6) Tsunekawa, S.; Ishikawa, K.; Li, Z. Q.; Kawazoe, Y.; Kasuya, A. *Phys. Rev. Lett.* **2000**, *85*, 3440.
(7) Trovarelli, A. In *Catalytic Science Series*, Vol. 2; Trovarelli, A., Ed.; Imperial College Press: London, 2002; p 15.
(8) (a) Chakraverty, S.; Mitra, S.; Mandal, K.; Nambissan, P. M. G.; Chattopadhyay, S. *Phys. Rev. B* **2005**, *71*, 024115. (b) Dutta, S.; Chattopadhyay, S.; Jana, D.; Banerjee, A.; Manik, S.; Pradhan, S. K.; Sutradhar, M.; Sarkar, A. *J. Appl. Phys.* **2006**, *100*, 114328. (c) Sachdeva, A.; Chavan, S. V.; Goswami, A.; Tyagi, A. K.; Pujari, P. K. *J. Solid State Chem.* **2005**, *178*, 2062. (d) Dannefaer, S.; Bretagnon, T.; Kerr, D. *J. Appl. Phys.* **1993**, *74*, 884.
(9) Catlow, C. R. A. *J. Chem. Soc., Faraday Trans.* **1990**, *86*, 1167.

JA808433D